

Aromatic Nitrogen Mustard-Based Autofluorescent Amphiphilic Brush Copolymer as pH-Responsive Drug Delivery Vehicle

Biswajit Saha, Neha Choudhury, Soma Seal, Bhuban Ruidas, and Priyadarsi De

Biomacromolecules, Just Accepted Manuscript • DOI: 10.1021/acs.biomac.8b01468 • Publication Date (Web): 06 Dec 2018

Downloaded from <http://pubs.acs.org> on December 7, 2018

Just Accepted

“Just Accepted” manuscripts have been peer-reviewed and accepted for publication. They are posted online prior to technical editing, formatting for publication and author proofing. The American Chemical Society provides “Just Accepted” as a service to the research community to expedite the dissemination of scientific material as soon as possible after acceptance. “Just Accepted” manuscripts appear in full in PDF format accompanied by an HTML abstract. “Just Accepted” manuscripts have been fully peer reviewed, but should not be considered the official version of record. They are citable by the Digital Object Identifier (DOI®). “Just Accepted” is an optional service offered to authors. Therefore, the “Just Accepted” Web site may not include all articles that will be published in the journal. After a manuscript is technically edited and formatted, it will be removed from the “Just Accepted” Web site and published as an ASAP article. Note that technical editing may introduce minor changes to the manuscript text and/or graphics which could affect content, and all legal disclaimers and ethical guidelines that apply to the journal pertain. ACS cannot be held responsible for errors or consequences arising from the use of information contained in these “Just Accepted” manuscripts.

Aromatic Nitrogen Mustard-Based Autofluorescent Amphiphilic Brush Copolymer as pH-Responsive Drug Delivery Vehicle

Biswajit Saha,^a Neha Choudhury,^a Soma Seal,^b Bhuban Ruidas,^c and Priyadarsi De^{a,*}

^a*Polymer Research Centre and Centre for Advanced Functional Materials, Department of Chemical Sciences, ^bDepartment of Biological Sciences, Indian Institute of Science Education and Research Kolkata, Mohanpur - 741246, Nadia, West Bengal, India.*

^c*Centre for Healthcare Science and Technology, Indian Institute of Engineering Science and Technology, Shibpur - 711103, West Bengal, India.*

* Corresponding Author: E-mail: p_de@iiserkol.ac.in

ABSTRACT: Delivery of clinically approved nonfluorescent drugs is facing challenges because it is difficult to monitor the intracellular drug delivery without incorporating any integrated fluorescence moiety into the drug carrier. The present investigation reports the synthesis of a pH-responsive autofluorescent polymeric nano-scaffold for the administration of nonfluorescent aromatic nitrogen mustard chlorambucil (CBL) drug into the cancer cells. Copolymerization of poly(ethylene glycol) (PEG) appended styrene and CBL conjugated *N*-substituted maleimide monomers enables the formation of well-defined luminescent alternating copolymer. These amphiphilic brush copolymers self-organized in aqueous medium into 25-68 nm nanoparticles, where the CBL drug is enclosed into the core of the self-assembled nanoparticles. *In vitro* studies revealed ~70% drug was retained under physiological conditions at pH 7.4 and 37 °C. At endolysosomal pH 5.0, 90% of the CBL was released by the pH-induced cleavage of the aliphatic ester linkages connecting CBL to the maleimide unit. Although the nascent nanoparticle (without drug conjugation) is nontoxic, the drug conjugated nanoparticle showed higher toxicity and superior cell killing capability in

1
2
3 cervical cancer (HeLa) cells rather than in normal cells. Interestingly, the copolymer without
4 any conventional chromophore exhibited photoluminescence under UV light irradiation due
5 to the presence of “through-space” π - π interaction between the C=O group of maleimide unit
6 and the adjacent benzene ring of the styrenic monomer. This property helped us intracellular
7 tracking of CBL conjugated autofluorescent nanocarriers through fluorescence microscope
8 imaging. Finally, the 4-(4-nitrobenzyl)pyridine (NBP) colorimetric assay was executed to
9 examine the ability of CBL-based polymeric nanomaterials towards alkylation of DNA.
10
11
12
13
14
15
16
17
18
19
20
21
22

23 **KEYWORDS:** Autofluorescent polymer, chlorambucil, drug delivery, cell imaging, DNA
24 alkylation
25
26
27
28
29
30

31 INTRODUCTION

32
33 Despite having several potential anticancer agents, the clinical payoff still remains inadequate
34 because of their severe host toxicity.^{1,2} The best permissible way to diminish toxicity is to
35 develop a technology for a controlled targeted drug delivery system (DDS) and release to
36 eradicate cancer cells while sparing normal cells. Currently, chemotherapy is still considered
37 as the most common method to treat numerous forms of cancer. Among all the existing
38 chemotherapeutic agents, alkylating agents were the first compounds identified to be useful
39 for cancer chemotherapy, because of their deoxyribonucleic acid (DNA) damaging ability by
40 virtue of DNA cross-linking, mispairing of bases etc.³ In this regard, nitrogen mustards have
41 emerged as suitable candidates for cancer therapy owing to their ability to form reactive
42 aziridinium ring by intramolecular displacement of chloride ion by the amine nitrogen.⁴
43
44 Among all types of nitrogen mustards, chlorambucil (CBL) has been extensively utilized for
45 cancer therapy, especially chronic lymphocytic leukemia (CLL).⁵ CBL is a clinically
46
47
48
49
50
51
52
53
54
55
56
57
58
59
60

1
2
3 approved bifunctional alkylating agent and it is worth to mention that the carboxylic side
4 chain of CBL is pharmacokinetic but not dynamic.⁶ Therefore, incorporation of a non-toxic
5 delivery system to the carboxylic side chain will only affect its absorption and half-life, not
6 the effectiveness.⁷ The major drawback to the use of CBL is that it is nonfluorescent,⁸ thus
7 prevent the tracking of intracellular drug delivery through fluorescence microscopy, as a
8 consequence, it will be difficult to have a knowledge regarding cellular drug uptake.
9

10
11
12 The recent past has witnessed the attachment of a fluorescent tag into the drug delivery
13 vehicle to aid in the analysis of the intracellular distribution of nonfluorescent drugs. Several
14 kinds of a fluorescent moiety such as coumarin,⁹ spiropyran-coumarin,¹⁰ carbazole¹¹ have
15 been reported to assist in the tracking of intracellular drug delivery. However, these current
16 approaches still suffer from limitations, notably low drug loading capabilities, water
17 solubility etc. Also, the addition of a fluorophore to a nonfluorescent drug may alter its
18 intracellular distribution.¹² Thus, to eliminate such concerns without affecting the
19 performance of the drug, new approaches should be developed. Typically, the material with
20 the ability to conquer these bottlenecks should; (i) have more number of conjugation sites to
21 have high drug loading capacity, (ii) possess high water solubility and low toxicity, and (iii)
22 not hamper the cellular uptake ability of the drug. Integration of all these facets is not trivial,
23 and hence till date, there is no report of any DDS satisfying all the above features in the
24 context of the delivery of nonfluorescent drugs. These necessitate the development of
25 different kinds of prodrugs which can provide the above prerequisites.
26
27
28
29
30
31
32
33
34
35
36
37
38
39
40
41
42
43
44
45
46
47
48
49

50 Existing literature helps us to find out the compound which can meet all the criteria; (i)
51 to (iii). Stimuli-responsive polymeric prodrugs may be potentially useful in this regard, as
52 they afford great therapeutic efficacy, a high percentage of drug loading capacity,¹³ controlled
53 drug release and selective recognition of the tumor microenvironment to target the cancer
54 cells avoiding the undesired side effects.¹⁴ These intelligent carriers release their payload as a
55
56
57
58
59
60

1
2
3 counter interaction with intracellular stimuli such as temperature,¹⁵ pH,^{16,17} redox,^{7,18}
4
5 enzyme,¹⁹ etc. Amongst the several types of stimuli-responsive system, the pH-sensitive
6
7 DDSs have earned a significant amount of attention as the pathological cells has more acidic
8
9 microenvironment relative to the normal cells.¹⁴ After addressing all the issues, we believe
10
11 that the last key point can also be responded by the use of an autofluorescent polymer.
12
13 Fortunately, nowadays researchers are keenly interested in developing different kinds of
14
15 luminescent polymers namely, poly(amido amine) (PAMAM),²⁰ poly(amino ester)s (PAE),²¹
16
17 poly(ether amide)s (PEA),²² poly[(maleic anhydride)-*alt*-(vinyl acetate)] (PMV),²³
18
19 poly(maleic anhydride-*alt*-styrene),²⁴ which could emit strong fluorescence in proper
20
21 conditions without having conjugated polymeric building block and conventional
22
23 fluorophores. Henry and co-workers reported pH-responsive and membrane destabilizing
24
25 polymeric carriers based on poly(maleic anhydride-*alt*-styrene) copolymers for intracellular
26
27 drug delivery.²⁵ Recently, we also reported such kind of unorthodox luminescent alternating
28
29 copolymer based on strictly alternating poly(maleimide-*alt*-styrene) skeleton, which can
30
31 exhibit blue fluorescence in varieties of solvents, and pH- and thermo-responsive
32
33 hydrophilic-hydrophobic phase transition in an aqueous medium. Generation of fluorescence
34
35 from this non-conjugated polymeric structure was attributed to the “through-space” π - π
36
37 communication between the C=O group of maleimide unit and adjacent benzene ring of the
38
39 styrenic monomer.^{26,27} This unconventional macromolecular luminogen as fluorescence
40
41 probe was used for selective and sensitive detection of picric acid (PA) with an instantaneous
42
43 response in 100% aqueous solution.²⁷
44
45
46
47
48
49
50
51

52 The objective of this contribution is to provide a first proof-of-concept to utilize the
53
54 autofluorescence property for intracellular tracking of DDS by fluorescence microscope
55
56 imaging from the poly(maleimide-*alt*-styrene) skeleton, connected to nonfluorescent drug
57
58 CBL through a pH-sensitive aliphatic ester linkage and biocompatible poly(ethylene glycol)
59
60

(PEG) chains. To this end, we have synthesized well-defined amphiphilic alternating brush copolymers by the sequence-specific copolymerization of two rationally designed monomers, PEG bearing styrene and CBL conjugated *N*-substituted maleimide *via* reversible addition-fragmentation chain transfer (RAFT) polymerization. We hypothesize that PEG attachment to the one segment of the copolymer will confer aqueous solubility, protein resistance property,²⁸ and biocompatibility to the alternating copolymer, widely observed for PEGylated systems.²⁹ The polymer self-assembled to a stable (at neutral pH) nanoparticle in aqueous solution with CBL drug moieties into the core which is surrounded by long PEG chains, thereby diminishing premature drug leakage and discriminating between cancer and healthy tissues. Cellular internalization of the CBL conjugated nanocarrier was confirmed by fluorescence imaging analysis and *in vitro* studies exhibited that the self-assembled nanocarriers were found to deliver their payloads upon contact with intracellular stimuli. Furthermore, the alkylation activity of CBL nitrogen mustard containing copolymer was performed spectroscopically by using a DNA model, 4-(4-nitrobenzyl)pyridine (NBP),³⁰ a colorimetric indicator for carcinogenic alkylating agents. To the best of our knowledge, this is the first report of synthesis of a DDS for nonfluorescent CBL drug, which could meet all the aforesaid criteria, thus opens up a new opportunity in the engineering of the autofluorescent amphiphilic copolymer for anticancer drug administration in cancer therapy.

EXPERIMENTAL SECTION

Materials. Furan (98%, Spectrochem, India), ethanolamine (Spectrochem, 99%), maleic anhydride (Loba Chemicals, 99%), dicyclohexylcarbodiimide (DCC, 99%, Aldrich), 4-(dimethylamino)pyridine (DMAP, 99%, Aldrich), 4-vinylbenzyl chloride (4-VBC, 90%, Fluka), *p*-toluenesulfonyl chloride (*p*-TsCl, 99%, Fluka), polyethylene glycol (PEG₂₀₀₀, 2000 g/mol, 99%, Aldrich), tetrabutylammonium chloride (Bu₄NCl, 99%, Aldrich), sodium

1
2
3 hydride (NaH, 99%, Aldrich), chlorambucil (CBL, Aldrich), HPLC water (Sisco Research
4 Laboratories Pvt. Ltd., India), sodium chloride (99%, Merck), sodium hydroxide (NaOH,
5 99%, Merck), triethylamine (TEA, 99%, Merck), anhydrous sodium sulphate (99%, Merck)
6 and sodium bicarbonate (99%, Merck) were used as received. 2,2'-Azobis(2-
7 methylpropionitrile) (AIBN, 98%, Aldrich) was recrystallized from methanol prior to use.
8 1,4-Dioxane (99%, Aldrich) was passed through a basic alumina column. The 2-
9 dodecylsulfanylthiocarbonylsulfanyl-2-methyl-propionic acid (DMP) was synthesized
10 following previous literature report.²⁶ Synthesis, purification and characterization of various
11 intermediates (Figure S1 to Figure S6) and monomers are provided in the Supporting
12 Information. NMR solvents such as CDCl₃ (99.8% D), DMSO-*d*₆ (99% D) and D₂O (99% D)
13 were purchased from Cambridge Isotope Laboratories, Inc., USA. Dry methanol,
14 dichloromethane (DCM) and tetrahydrofuran (THF) were prepared by following standard
15 procedures. Solvents such as toluene, hexanes (mixture of isomers), diethyl ether, DCM,
16 isopropanol were purchased from Merck and used as received without any further
17 purification. Cervical cancer cells (HeLa) and human breast cancer cells (MCF-7) were
18 maintained in Dulbecco's Modified Eagle Medium (DMEM, Thermo Fisher Scientific).
19 Human embryonic kidney cells 293 (HEK 293) were maintained in Minimum Essential
20 Medium (MEM, Thermo Fisher Scientific) containing 10% (v/v) fetal bovine serum (FBS,
21 Gibco, Thermo Fisher Scientific) and 1% penicillin-streptomycin (Thermo Fisher Scientific)
22 at 37 °C under a 5% CO₂ humidified atmosphere. Cells were washed with PBS, trypsinized
23 using 0.25% trypsin (Thermo Fisher Scientific) and seeded in 24-well flat-bottomed plastic
24 plates (Nunc) for all assays. The 3-(4,5-dimethylthiazol-2-yl)-2,5-diphenyltetrazolium
25 bromide (MTT) and dimethyl sulfoxide (DMSO, 99.9%, cell culture grade) were purchased
26 from USB corporation and Ameresco, respectively.
27
28
29
30
31
32
33
34
35
36
37
38
39
40
41
42
43
44
45
46
47
48
49
50
51
52
53
54
55
56
57
58
59
60

1
2
3 **Instruments and Characterizations.** The detail instrumentation of size exclusion
4 chromatography (SEC), ¹H NMR, UV-Vis and fluorescence spectroscopy can be found in our
5 earlier report.²⁷ The fluorescence quantum yield (ϕ_F) in solution was determined using
6 quinine sulfate in 0.05 M sulphuric acid ($\phi_F = 52\%$) as a standard. Positive mode electrospray
7 ionization mass spectrometry (ESI-MS) was performed on a Q-ToF Micro YA263 high
8 resolution (Waters Corporation) mass spectrometer. Matrix-assisted laser
9 desorption/ionization time-of-flight (MALDI-TOF) mass spectrometry was carried out on a
10 Bruker UltrafleXtreme™ instrument equipped with a smart beam-II laser in the reflector
11 mode and an acceleration voltage of 22 kV. Dynamic light scattering (DLS) measurements
12 were carried out at room temperature in a Malvern Zetasizer Nano instrument equipped with
13 a He–Ne laser system operating at 633 nm (scattering angle = 173°). Polymer solutions (1.0
14 mg/mL) were filtered through a 0.45 μm syringe filter prior to measurements. Field emission-
15 scanning electron microscopy (FE-SEM) study was performed on a Carl Zeiss Sigma SEM
16 instrument. The TEM images were recorded in a JEOL JEM-2100F instrument at 200 kV
17 operational mode to visualize the morphologies of the nanoparticles. Samples for TEM were
18 prepared by drop-casting an aqueous solution (1 mg/mL) on a carbon coated Cu-grid and then
19 dried for few hours under vacuum at room temperature. An epifluorescence Olympus IX81
20 model equipped with plan fluorite objective with 40X magnification was used to obtain
21 fluorescence images.

22
23
24 **Procedure for the synthesis of alternating brush copolymers, BPDC1-BPDC3.**

25 Typically, **M1**, **M2**, DMP, AIBN, and 1,4-dioxane were sealed in a 20 mL reaction vial
26 equipped with a magnetic stir bar. The vial was sealed tightly, placed on an ice-water bath
27 followed by purging with dry N₂ for 20 min. Next, the reaction vial was kept in a preheated
28 polymerization block at 70 °C for 24 h, after which the reaction was quenched by cooling it
29 on an ice-water bath and exposing to air. Then, the unreacted PEG macromonomer and
30

1
2
3 maleimide monomer were removed by pouring the reaction mixture into a large excess of
4 diethyl ether, followed by centrifuging the resultant cloudy dispersion at 3500 rpm for 15
5 min. The upper portion of the diethyl ether layer was carefully decanted. This was repeated
6 six times with a fresh batch of diethyl ether each time. Then, the purity of the resultant
7 polymer was verified by ^1H NMR spectroscopy (Figure 1C). Polymerization reactions were
8 carried out at different feed ratios of $[\mathbf{M1} + \mathbf{M2}] : \text{DMP} : \text{AIBN} = 50/100/200 : 1 : 0.5$.
9 Molecular weights and dispersity (D) values of all the resulting polymers are summarized in
10 Table S1.
11
12
13
14
15
16
17
18
19
20

21 In addition, we have synthesized a copolymer without incorporation of CBL (Scheme
22 S1). Briefly, 2-hydroxyethyl maleimide (HEMI, 13.3 mg, 0.094 mmol), $\mathbf{M2}$ (200 mg, 0.094
23 mmol), DMP (0.7 mg, 0.002 mmol), and AIBN (0.164 mg, 0.001 mmol, from stock solution)
24 were dissolved in 1,4-dioxane in a 20 mL septa sealed reaction vial equipped with a magnetic
25 stir bar. The vial was purged with N_2 for 20 min, and placed in a preheated reaction block at
26 70 °C for 24 h. Purification of the resultant polymer was executed using the same above
27 mentioned procedure.
28
29
30
31
32
33
34
35
36
37

38 **Self-assembly study.** Self-assembly of the resultant brush copolymers (\mathbf{BPDCx}) was
39 performed by dissolving the polymer in de-ionized (DI) water. Typically, 5 mg of each
40 polymer was dissolved in 1 mL of DI water, a selective solvent for the PEG segment. The
41 resulting solution was allowed to stir for overnight. Size distribution and morphology of the
42 self-assembled polymeric nanoaggregates were determined by DLS measurement, FE-SEM
43 and TEM study at a concentration of 1.0 and 0.1 mg/mL, respectively.
44
45
46
47
48
49
50
51

52 **pH-Triggered degradation of $\mathbf{BPDC2}$ polymeric nanoaggregates.** The hydrolysis of
53 the ester linkage of $\mathbf{BPDC2}$ polymeric aggregates was determined by DLS method *via*
54 measuring the hydrodynamic size distribution value. Briefly, the pH values of self-assembled
55 $\mathbf{BPDC2}$ polymeric nanoaggregates (2.0 mg/mL) were adjusted to 7.4 and 5.0. After being
56
57
58
59
60

1
2
3 hydrolyzed at room temperature for predetermined time intervals, the hydrodynamic
4 diameter, D_h , of hydrolyzed polymer solutions were measured by DLS study. Also, after
5
6 different incubation time intervals, aliquots (20 μ L) were taken out for FE-SEM and TEM
7
8
9 measurements.

10
11
12
13 ***In vitro* drug release.** The performance of drug delivery was measured in both neutral
14 and acidic environment. For the neutral condition, **BPDC2** was dissolved in DI water (1
15 mg/mL) and sealed in a 2000 Da cut-off dialysis bag. Then, the dialysis bag was immersed in
16
17 50 mL of phosphate buffered saline (PBS) solution at pH 7.4 at 37 °C with a magnetic stir
18
19 bar. At each predetermined time point, 2 mL of the PBS solution was removed and the
20
21 release of chlorambucil was determined by measuring its absorbance at 260 nm by UV-Vis
22
23 spectroscopy. For the acidic condition, buffer solutions (pH = 6.4 and 5.0) were used as the
24
25 release medium at 37 °C.
26
27
28
29
30
31

32 **Cell viability assay (MTT assay).** The cytotoxicity of free CBL, CBL conjugated
33 polymeric nanoparticles and polymeric nanoparticle alone was studied in HEK 293 and HeLa
34 cell lines using tetrazolium salt, MTT. In a 24-well plate, 5×10^4 cells were seeded per well
35 with 1.0 mL DMEM containing 10% FBS and allowed to adhere for 24 h. CBL conjugated
36
37 polymeric nanoparticles and polymeric nanoparticle alone are dissolved in PBS to perform
38
39 the cytotoxicity assay, whereas free CBL was dissolved in DMSO as it is hydrophobic in
40
41 nature. Prior to drug treatment, media from the cells was aspirated, and replaced with fresh
42
43 media. Then, various concentration of free CBL, drug conjugated polymeric nanoparticles
44
45 and nascent polymeric nanoparticles were added to the wells. Cells were incubated for 24 h at
46
47 37 °C with 5% CO₂. Control cells received equal volume of vehicle and were incubated for
48
49 the same time period. All experiments were run in triplicate. After 24 h, 100 μ L freshly
50
51 prepared solution of MTT (5 mg/mL) was added to each well and incubated for 4 h.
52
53 Following incubation media was then aspirated from the cells, and the purple formazan
54
55
56
57
58
59
60

1
2
3 crystals that formed as a result of the reduction of MTT by mitochondrial dehydrogenase
4 enzyme from the cells were dissolved in 500 μL of DMSO (added per well). After 10 min,
5 the absorbance from formazan crystals was measured at 570 nm. Similar experiments were
6 also performed in HEK 293 cell line with free CBL, CBL conjugated nanoparticle and
7 nanoparticle alone.

8
9
10
11
12
13
14
15 **Cell imaging study.** HeLa and MCF-7 cells were cultured on the coverslip for 24 h at
16 37 $^{\circ}\text{C}$ with 5% CO_2 . Then, the cells were treated with **BPDC2** (drug concentration = 14
17 $\mu\text{g}/\text{mL}$) and incubated for 24 h at 37 $^{\circ}\text{C}$. The imaging process was performed after cells were
18 washed with PBS buffer and mounted on a glass slide. Fluorescence images were acquired
19 through a high-resolution epifluorescence microscope with 40X objective lens (Nikon Eclipse
20 Ti-S, inverted microscopes) under blue, green and red channels.

21
22
23
24
25
26
27
28
29
30 **NBP alkylation assay.** Alkylation activity of aromatic nitrogen mustard of
31 chlorambucil in **BPDC2** has been investigated with 4-(4-nitrobenzyl)pyridine (NBP) by
32 following the established procedure with some modifications.³¹ **BPDC2** was dissolved in
33 Milli-Q water (1.0 mg/mL) in a septa sealed vial. The vial was placed in an ice-water bath at
34 0 $^{\circ}\text{C}$. A 1.0 mL aliquot of 0.2 M NaOAc buffer pH 5.0 was added, followed by addition of 40
35 μL 0.5 M NBP in acetone. Then, the resulting solution was heated to 100 $^{\circ}\text{C}$ for 20 min.
36 After cooling the reaction mixture to room temperature, 2.0 mL of triethylamine/acetone
37 (1:1) was added. The solution was diluted to 10 mL with acetone and shaken by a hand mixer
38 for 1 min. Afterwards, the absorbance of the violet color solution was measured at 560-570
39 nm by UV-Vis spectroscopy within an hour. The rate constant of the reaction was calculated
40 by the following equation (1):

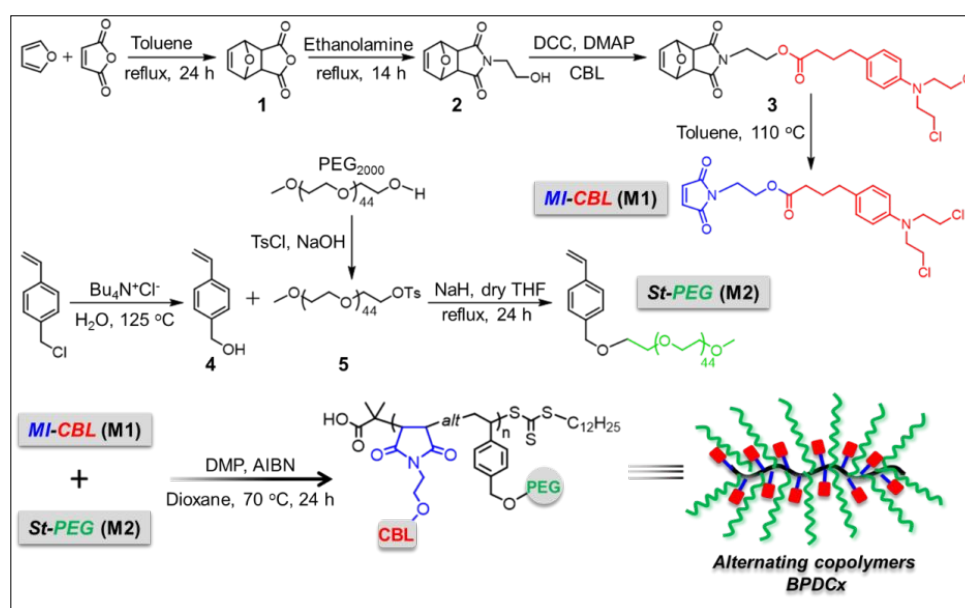
$$\ln \frac{A_{\infty} - A_0}{A_{\infty} - A_t} = kt \quad (1)$$

1
2
3 Where A_0 is the initial absorbance, A_∞ denotes the absorbance of the adduct when all NBP
4 has been consumed, A_t is the absorbance at different time intervals and k (rate constant) is the
5 slope of the $\ln\{(A_\infty - A_0)/(A_\infty - A_t)\}$ versus time (t) plot.
6
7
8
9

10 11 12 13 14 RESULTS AND DISCUSSION

15
16 **Synthesis and characterization of nitrogen mustard-based amphiphilic alternating**
17 **copolymer.** Since polymerization of an equimolar mixture of styrene and maleimide gives
18 rise to strictly alternating poly(maleimide-*alt*-styrene) skeleton,³² in the present study
19 amphiphilic alternating brush copolymer was synthesized by the copolymerization of
20 chlorambucil functionalized maleimide derivative (MI-CBL, **M1**) and PEG conjugated
21 styrene macromonomer (St-PEG, **M2**) as shown in Scheme 1. The **M1** and **M2** monomers
22 were synthesized through multistep reactions as shown in Scheme 1. Maleic anhydride was
23 converted into 4,10-dioxatricyclo[5,2,1,0,2,6]dec-8-ene-3,5-dione (**1**, Figure S1) *via* Diels-
24 Alder reaction with furan, and it was subjected to react with ethanolamine to give compound
25 **2** (Figure S2). Compound **2** was then coupled with CBL *via* dicyclohexylcarbodiimide (DCC)/
26 4-(dimethylamino)pyridine (DMAP) esterification reaction to produce the compound **3**
27 (Figure S3). The final monomer **M1** was synthesized through retro Diels-Alder reaction of
28 compound **3** in toluene at 110 °C. The formation of **M1** was characterized using ¹H NMR
29 spectroscopy (Figure 1A) and mass analysis (Figure S4). To synthesize the second monomer
30 (**M2**), at first 4-vinylbenzyl chloride (4-VBC) was converted into its alcohol derivative (**4**,
31 Figure S5) using a phase transfer catalyst in water at 125 °C.³³ Polyethylene glycol
32 monomethyl ether (molecular weight = 2000 g/mol) was treated with tosyl chloride to yield
33 PEG₂₀₀₀ tosylate (**5**, Figure S6). Compounds **4** and **5** were then reacted together in presence of
34 sodium hydride (NaH) in dry tetrahydrofuran (THF) to produce PEG functionalized styrenic
35 macromonomer **M2**. The successful synthesis of **M2** was confirmed by both ¹H NMR
36
37
38
39
40
41
42
43
44
45
46
47
48
49
50
51
52
53
54
55
56
57
58
59
60

spectroscopy (Figure 1B) and matrix-assisted laser desorption/ionization time-of-flight (MALDI-TOF) mass spectrometry (Figure 1D). MALDI-TOF mass spectrum of **M2** showed a series of peaks, where two major signals are separated by exactly 44 m/z value, which is identical with the molar mass of ethylene glycol (-O-CH₂-CH₂-) repeating unit. Furthermore, we performed size exclusion chromatography (SEC) analysis of **M2** (Figure S7), where we observed monomodal molecular weight distribution. These results suggest the formation PEG appended styrenic macromonomer **M2**.



Scheme 1. Synthetic routes employed for the preparation of maleimide conjugated chlorambucil monomer (**M1**), styrenic macromonomer (**M2**) and pH-responsive amphiphilic alternating copolymer, **BPDC_x**, *via* RAFT polymerization.

Subsequently, copolymerization reactions of **M1** and **M2** were carried out using AIBN as an initiator and DMP as chain transfer agent (CTA) in 1,4-dioxane at 70 °C *via* RAFT polymerization (Scheme 1). The use of RAFT polymerization can offer unprecedented latitude in the synthesis of water-soluble amphiphilic architectures with precise molecular weight and appropriate functionality for the encapsulation or attachment of therapeutic agents.^{34,35} The copolymers were named as **BPDC_x**, where x represents the different feed

1
2
3 ratios of **M1** and **M2** (**BPDC1-BPDC3**, Table S1). The CTA to initiator ratio $[CTA]/[AIBN]$
4
5 = 1:0.5 was kept constant during all the polymerization reactions. After purification,
6
7 copolymers were characterized by 1H NMR spectroscopy and a typical 1H NMR spectrum of
8
9 **BPDC2** is shown in Figure 1C, where the absence of vinyl and maleimide proton peaks
10
11 ensures the purity of the resulting polymer. Formation of the copolymer was also confirmed
12
13 by MALDI analysis. Increase in the molecular mass distribution of **M2** after RAFT
14
15 polymerization with **M1** approves the attachment of both the monomers into the polymer
16
17 chain (Figure 1D). The number average molecular weight ($M_{n,SEC}$) and molecular weight
18
19 distribution (dispersity, D) values of the copolymers were evaluated by SEC in THF and
20
21 results are summarised in Table S1. SEC plots (Figure S7) of **BPDCx** polymers showed
22
23 unimodal molecular weight distributions with a small trace of unreacted non-functionalized
24
25 PEG (Figure S7). The elution volume of the polymers decreases with the increase of
26
27 $[monomer (M)]/[CTA]$ ratio in the feed. However, the measured $M_{n,SEC}$ values are much
28
29 lower compared to the theoretical number average molecular weight ($M_{n,theo}$) values (Table
30
31 S1). This is most probably due to the different hydrodynamic volume of synthesized
32
33 polymers than that of poly(methyl methacrylate) (PMMA) standards, which we have used to
34
35 construct the conventional calibration for the calculations of $M_{n,SEC}$ values from SEC analysis.
36
37
38
39
40
41

42 Several literature reports,^{36,37} and also our earlier work²⁶ revealed the formation of
43
44 perfectly alternating sequences of monomers throughout the polymer chain upon
45
46 copolymerization of maleimide and styrene or their derivatives. The integration ratio of the
47
48 aromatic peak of CBL moiety at 6.60 ppm and methoxy proton of PEG entity at 3.36 ppm is
49
50 almost equal to one (Figure 1C), suggesting a strong propensity of alternating
51
52 copolymerization of these monomers. The alternate sequence of the monomers was further
53
54 ascertained by MALDI-TOF analysis (Figure S8). Figure S8 revealed that the **BPDC2** is a
55
56
57
58
59
60

perfectly alternating copolymer, as there is no single molecular mass distribution which is equal to either the mass of **M1** or **M2**.

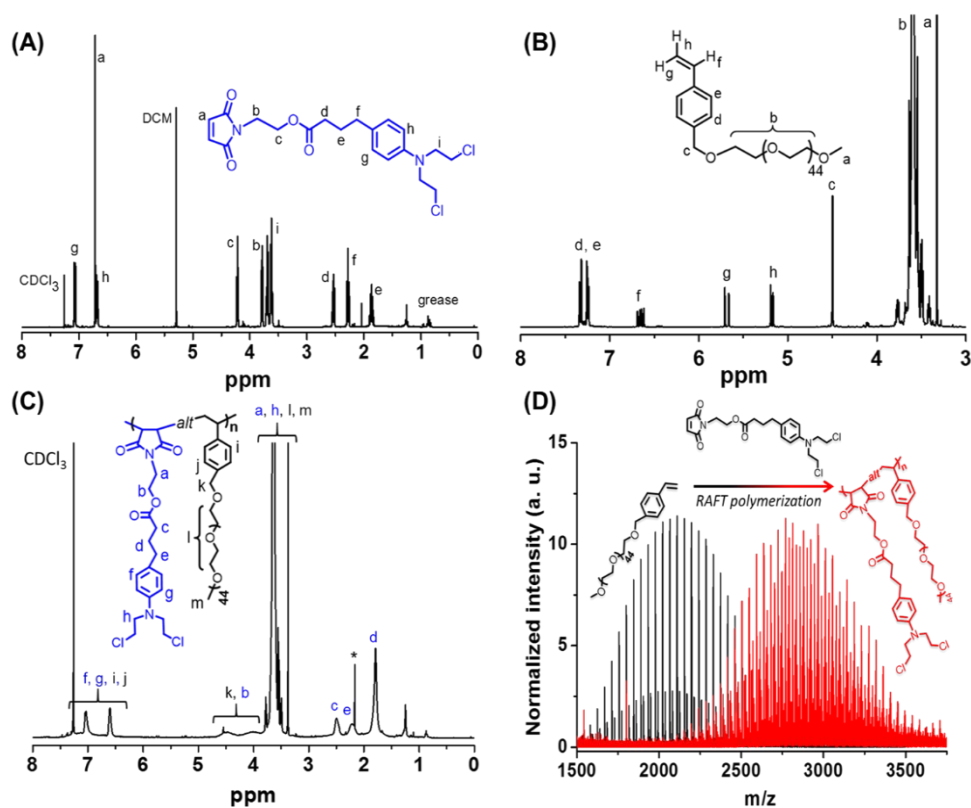
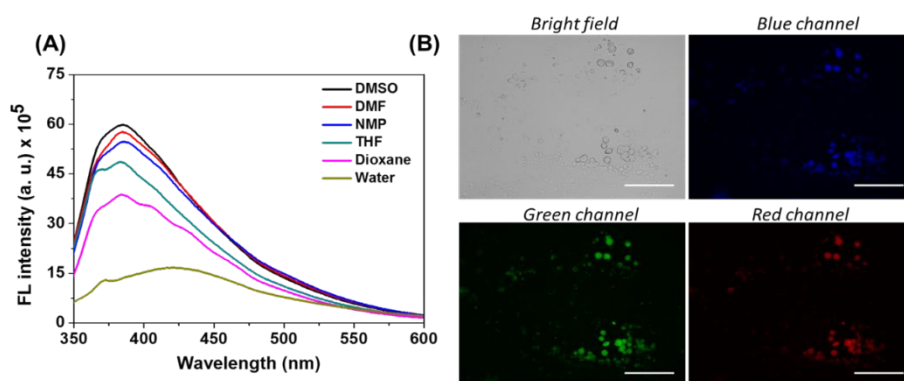


Figure 1. ¹H NMR spectra of (A) **M1**, (B) **M2**, and (C) **BPDC2** in CDCl₃. (D) MALDI-TOF mass spectra of **M2** before (black trace) and after (red trace) RAFT polymerization with **M1**.

Photophysical properties. Alternating copolymers based on poly(maleimide-*alt*-styrene) skeleton without having any conventional fluorophore moiety can exhibit fluorescence behaviour.^{26,38} Thus, the photophysical property of **BPDC2** was investigated in different solvents. The absorption spectra of **BPDC2** is represented in Figure S9, which displayed two absorption bands in the UV region at 258 and 304 nm, collectively attributed to the π - π^* and n - π^* electronic transitions of maleimide carbonyl²⁷ and chlorambucil moiety. Next, to probe the emission behaviour of **BPDC2**, the polymer solution was irradiated with UV ($\lambda_{\text{ex}} = 339$ nm) in different solvents (Figure 2A). A broad emission spectrum was observed with emission maxima at around 422 and 384 nm in water and various organic solvents, respectively. The fluorescence quantum yield (ϕ_F) of **BPDC2** in THF was estimated

1
2
3 to be 0.98%. The appearance of this kind of unanticipated fluorescence is due to the “through
4 space” π - π communication between the benzene ring and the neighbouring C=O group of
5
6
7
8 maleimide unit.²⁶ In the next step, luminescence characteristics of the **BPDC2** polymer were
9
10 studied by virtue of fluorescence microscopy. The **BPDC2** polymer was dissolved in water
11
12 (0.5 mg/mL), drop cast on a glass slide, dried overnight at ambient condition, followed by
13
14 vacuum drying. The fluorescence microscope images (Figure 2B and Figure S10) show that
15
16 the **BPDC2** polymer can exhibit blue, green and red emission on illumination with UV light
17
18 although no conventional fluorophore moiety was employed during the synthesis of
19
20 polymers.³⁹ Interestingly, the observed emission behaviour of the **BPDC2** polymer is in well
21
22 accordance with the PL spectra (Figure 2A).
23
24
25



26
27
28
29
30
31
32
33
34
35
36
37
38
39 **Figure 2.** (A) Fluorescence spectra ($\lambda_{\text{ex}} = 339$ nm) of **BPDC2** in different solvents, and (B)
40
41 fluorescence microscopy images of the **BPDC2**. The images were taken from blue (420-460
42
43 nm), green (510-550 nm) and red (575-625 nm) channels, respectively. Scale bar is 100 μm .
44
45

46 **Self-assembly of brush copolymers in aqueous medium.** It is well-documented that
47
48 amphiphilic brush copolymers with densely grafted macromolecular architectures in the
49
50 selective solvent can possess a variety of morphologies such as spherical micelles,⁴⁰
51
52 cylindrical nanostructures,⁴¹ multi-molecular micelle,⁴² etc. The generation of these higher-
53
54 order molecular assemblies is vastly dependent on the hydrophobicity/hydrophilicity ratios of
55
56 the copolymer compositions. Due to the presence of long PEG side chains, the as-synthesized
57
58 **BPDCx** polymers can quickly be dissolved in aqueous media without any external assistance
59
60

and endure self-assembly (Figure 3A). First, the self-assembly behaviour of **BPDC1-BPDC3** was investigated by dynamic light scattering (DLS) (Figure 3B-3D). The number-average hydrodynamic diameter (D_h) values were found to be 25 ± 5.0 (PDI = 0.265), 50 ± 2.0 (PDI = 0.230) and 68 ± 3.0 (PDI = 0.167) nm for **BPDC1**, **BPDC2**, and **BPDC3**, respectively, with a monomodal size distribution. The significant increase in D_h from 25 to 68 nm as a function of $[M]/[CTA]$ ratio can be described by the fact that with the increase of monomer feed into the copolymer composition, large number of hydrophobic (**M1**) and hydrophilic (**M2**) segment will accumulate into the core and corona of the nanoparticle, respectively, on self-assembly in water.

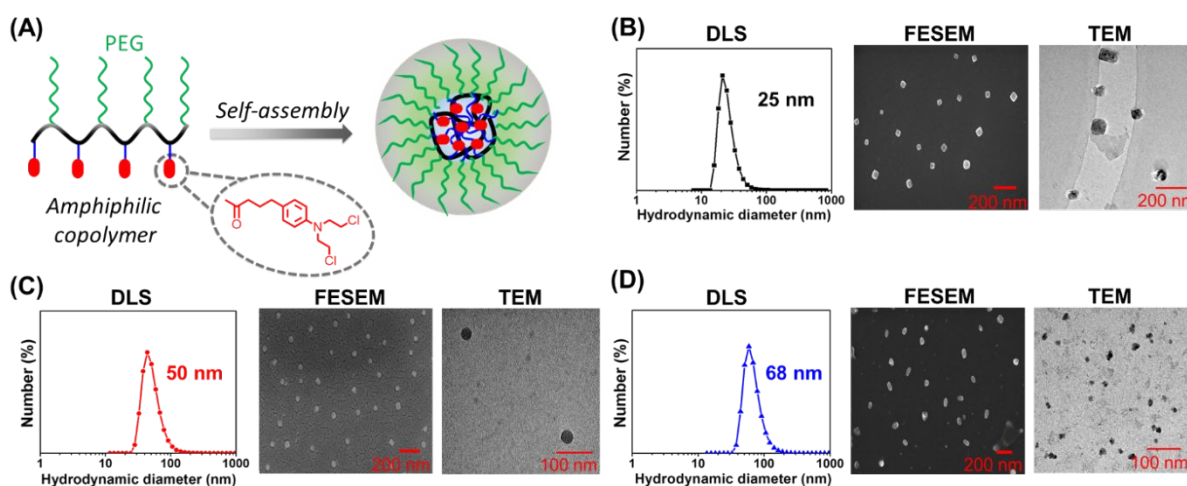


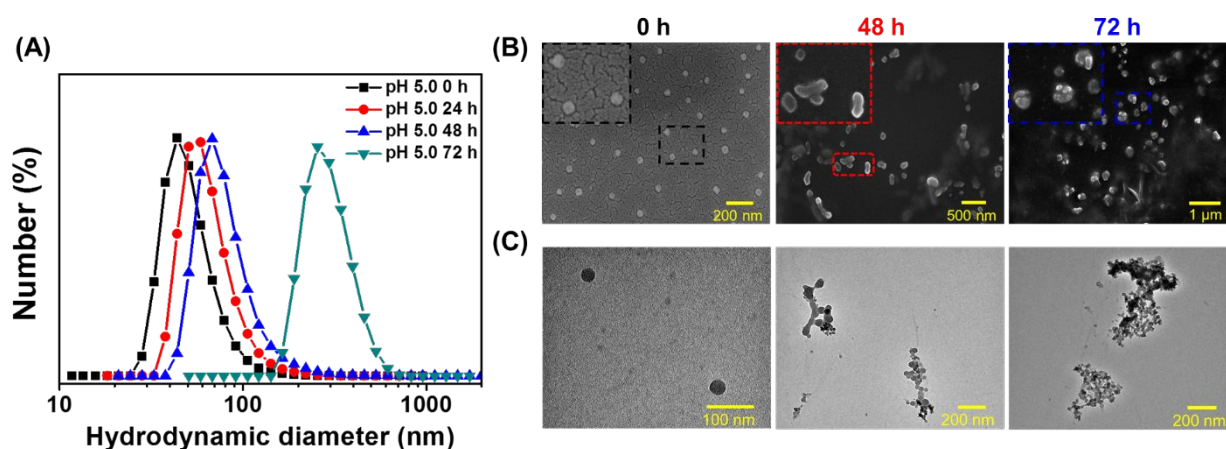
Figure 3. Schematic representation of self-assembly of **BPDCx** in an aqueous medium (A). DLS curves, FE-SEM and TEM images of (B) **BPDC1**, (C) **BPDC2**, and (D) **BPDC3**.

To gain more information on the formation and morphology of the **BPDCx** nanostructures in aqueous solutions, FE-SEM and TEM images were recorded. As shown in Figure 3B-3D, **BPDC1-BPDC3** brush copolymers self-assembled into square shaped, spherical and a mixture of spherical and non-spherical nanoparticles, respectively with an average size of 30 to 40 nm. Furthermore, the TEM images have confirmed the existence of different morphologies having a diameter in the range of 30 to 40 nm. Note that the apparent hydrodynamic diameters in aqueous medium obtained from DLS are somewhat larger in size

1
2
3 in comparison to the size measured from FE-SEM and TEM, because electron microscopy
4 study was done with dried samples, whereas in DLS measurements polymer chains are
5 hydrated with water molecules.^{43,44} Nevertheless, the abrupt change in morphologies by
6 varying chain length could be ascribed to the differences in hydrophobic MI-CBL chain
7 length and higher PEG grafting density. This observation demonstrates how using RAFT
8 polymerization to prepare brush copolymer by “grafting through” approach provides a handle
9 through which the morphology of the self-assembled nanoparticle can be manipulated. To
10 elucidate the mechanism of self-assembly behaviour of as-synthesized amphiphilic
11 copolymers, ¹H NMR spectroscopy was performed in two different solvents, CDCl₃, and D₂O
12 (Figure S11). The CDCl₃ is a good solvent for both the segments **M1** and **M2**, whereas D₂O
13 is a bad solvent for the **M1** units present in the polymer chain. The ¹H NMR spectrum of
14 **BPDC2** showed all the characteristics peaks from both the co-monomers in CDCl₃ (Figure
15 S11A), while the resonance signals corresponding to the CBL unit of **M1** is completely
16 vanished in D₂O (Figure S11B). These results describe the formation of higher-order
17 structures in water through the precise arrangement of hydrophobic (**M1**) and hydrophilic
18 (**M2**) components, where hydrophobic aggregation of the polymer skeleton including **M1**
19 unit and styrenic part of **M2** is surrounded by the long hydrophilic PEG chains.⁴⁵
20 Nevertheless, **BPDC2** spherical nanoparticle could be a better drug carrier to exploit the
21 enhanced permeability and retention (EPR) effect as it possesses the nanoscopic size of 50
22 nm, which is in between 10-100 nm.⁴⁶

23
24
25
26
27
28
29
30
31
32
33
34
35
36
37
38
39
40
41
42
43
44
45
46
47
48
49
50 **Acid-triggered activation of BPDC2 polymeric nanoparticles.** With the aliphatic
51 ester linkages connecting CBL moieties to the polymeric backbone, **BPDC2** is expected to
52 undergo hydrolysis under acidic conditions. Therefore, the sensibility of the polymer
53 nanoparticles containing the acid-labile ester groups was tested by DLS in an acidic buffer
54 (pH 5.0) at 37 °C. Upon incubating **BPDC2** in the acidic buffer for 0 to 48 h, the *D_h* values
55
56
57
58
59
60

1
2
3 increased from 25 to 82 nm with unimodal monodisperse size distribution (Figure 4A). After
4
5
6 72 h, a remarkable increase in size distribution ($D_h = 295$ nm) was observed, presumably due
7
8 to the formation of hydrophilic alcohol derivative on complete hydrolysis of the ester
9
10 linkages. In contrast, no significant change was observed in the DLS study when the **BPDC2**
11
12 was incubated at physiological pH 7.4 at 37 °C (Figure S12). This study confirms the pH-
13
14 responsiveness of the aliphatic ester linkages connecting CBL moieties to the polymer
15
16 skeleton, which can be readily cleaved by intracellular pH to deliver the drug.⁴⁷



21
22
23
24
25
26
27
28
29
30
31
32
33
34
35 **Figure 4.** (A) Analysis of number-average hydrodynamic diameter (D_h), (B) FE-SEM and,
36
37 (C) TEM images of **BPDC2** polymeric nanoparticles before and after hydrolysis at pH 5.0.

38
39
40
41 Additionally, pH-triggered degradation of **BPDC2** nanoparticles was further
42
43 corroborated by FE-SEM and TEM observations. Figure 4B and 4C reveal that with the
44
45 increase of incubation time from 0 to 72 h at pH 5.0, the spherical nanoparticles undergo
46
47 fusion with complete disruption of spherical morphologies, resulting in aggregated
48
49 nanostructures of higher sizes. This result is consistent with the appearance of higher size
50
51 distribution in DLS. The increase in particle size and size distribution, as shown by both
52
53 DLS, FE-SEM, and TEM are strong evidence of core-shell nanoparticle aggregation over
54
55 time.⁴⁸ We hypothesize that on hydrolysis of ester linkages, the CBL moieties released from
56
57
58
59
60

1
2
3 the nanoparticles, leading to an imbalance in hydrophobicity/hydrophilicity ratio and result in
4
5 particle aggregation.
6

7
8 **pH-responsive *in vitro* release studies.** To evaluate the potential of the present DDS,
9
10 *in vitro* drug release kinetics was studied *via* dialysis method.⁴⁹ For this purpose, **BPDC2** was
11
12 dissolved in de-ionized water (1 mg/mL) and it was sealed in the dialysis membrane (MWCO
13
14 = 2000 g/mol). Subsequently, the dialysis bag was immersed in a beaker containing 50 mL of
15
16 PBS buffer at pH 7.4 and 37 °C. The cumulative release of the cargo from the core of the
17
18 nanoparticles was determined using UV-Vis spectroscopy by measuring the absorbance at a
19
20 wavelength of 260 nm for 10 days. In PBS, **BPDC2** nanoparticles are displaying slow
21
22 rupturing process as a small amount of CBL (~32%) leached out within 10 days of
23
24 incubation. This observation assists us to claim that the synthesized polymeric nanocarrier are
25
26 quite stable under physiological conditions and able to stabilize the drug molecule during
27
28 prolonged circulation in blood. According to the chemical structure of the **BPDCx** polymer,
29
30 CBL was conjugated to the copolymer backbone through an aliphatic ester bond, which is
31
32 susceptible to cleave at endosomal pH (4.5-6.5) resulting in disruption of nanoscaffolds
33
34 leading to the delivery of the cargoes (CBL) to the intracellular environment (Figure 5A).⁴⁷
35
36 To demonstrate this effect, the *in vitro* drug release studies were performed by incubating
37
38 **BPDC2** in phosphate buffered saline at pH 6.4 and 5.0. The corresponding drug release
39
40 profiles are provided in Figure 5B. At pH 6.4, the percentage of drug release was increased
41
42 up to ~57% because of the ester hydrolysis at slightly acidic pH. The releasing phenomena
43
44 could be further accelerated up to ~90% by lowering the pH to 5.0. This fact can be attributed
45
46 to the facile cleavage of the ester bond from the side-chain of the copolymer at
47
48 endolysosomal pH. However, a significant difference in CBL releasing behaviour was seized
49
50 after 48 h of incubation which is mainly due to the substantial destabilization of the
51
52 nanocarrier as shown in DLS measurement (Figure 4A). Interestingly, the slow pH-
53
54
55
56
57
58
59
60

responsive feature of the newly engineered drug delivery vehicle makes them suitable for once-a-week administration as it releases the drug for more than 7 days in a sustained manner.⁵⁰ Thus, the present system could be of interest as a potential DDS where a long-lasting drug depot is desirable.

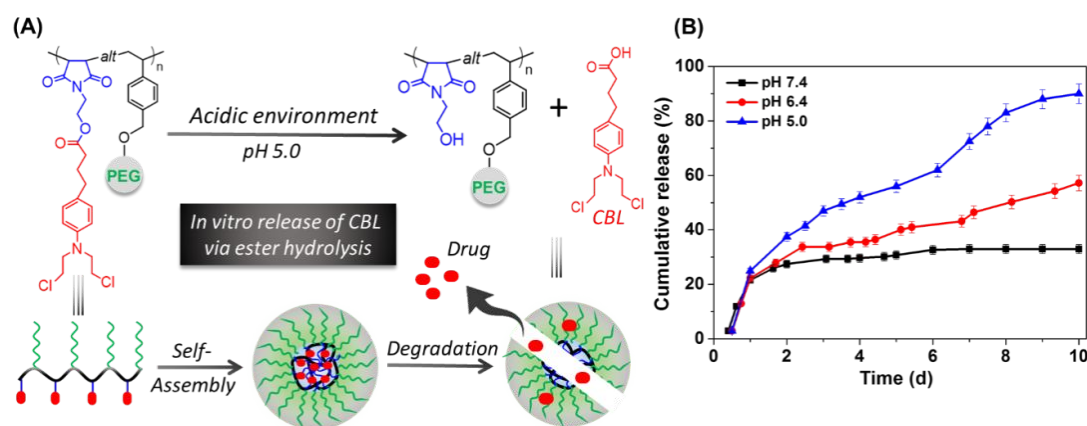


Figure 5. (A) Schematic representation of pH-triggered release of CBL from **BPDC2** nanocarrier. (B) Cumulative release profile of CBL from interior of the nanocarrier at varying pH.

Cytotoxicity studies. Having been demonstrated the pH-triggered release of payloads, in the following step, the intracellular drug delivery capability of **BPDC2** and the control alternating polymer without drug attachment (see **BPC** in Scheme S1) and free CBL were investigated by assessing the cytotoxicity in human embryonic kidney cells 293 (HEK 293) and cervical cancer (HeLa) cell lines using MTT assay.⁵¹ Both the normal and cancer cell lines were exposed to various drug concentrations present in the nanoparticles ranging from 0-28 $\mu\text{g/mL}$ (polymer concentration: 250 to 1000 $\mu\text{g/mL}$, 7 $\mu\text{g/mL}$ of CBL in 250 $\mu\text{g/mL}$ polymeric scaffold, the drug loading content is 9.29%) for 24 h at 37 $^{\circ}\text{C}$. The cytotoxicity results are shown in Figure 6A, where more than 75% cell viability is observed with **BPC** in both HEK 293 and HeLa cell lines even at a very high dose of 1000 $\mu\text{g/mL}$, indicating the biocompatibility of nascent polymeric scaffold for drug delivery applications. Similarly, the

1
2
3 **BPDC2** showed more than 70% cell viability in normal HEK 293 cell line, suggesting
4 nontoxic nature of the **BPDC2** towards the normal cells (Figure 6B), as a proof of which, the
5 cytotoxic assay of free CBL was carried out in HEK 293 cell lines where only 50% cell
6 viability was observed which is more toxic than the **BPDC2** nanoparticle (Figure 6C). The
7 drug concentration was maintained as equivalent to the drug conjugated nanoparticle.
8 Interestingly, in the HeLa cell line, the **BPDC2** nanoparticle exhibited superior cell killing
9 upto 60% and became highly effective to impart toxicity to the cancer cells (Figure 6B). This
10 could be due to the acidic environment of cancer cells compared to the normal cells, allowing
11 the better release of CBL through acid catalyzed ester hydrolysis.⁵² It should be noted that the
12 CBL conjugated polymeric nanoparticles exhibited about 40% killing of HeLa cells at a
13 concentration of 14 $\mu\text{g/mL}$, whereas there were almost no cell killing ($\sim 4\%$) phenomena
14 observed with free CBL (Figure 6C) which shows that our polymeric nanocarrier are more
15 effective to penetrate the cell membrane and induce their toxicity. However, a similar cell
16 viability was observed with free CBL in both HEK 293 ($\sim 60\%$) and HeLa ($\sim 51\%$) cell lines
17 at a concentration of 28 $\mu\text{g/mL}$. Nevertheless, the macromolecular drug carriers can also
18 show better uptake capacity into the cancer tissues *via* EPR effect compared to free drug.^{53,54}
19 Thus, the present *in vitro* investigation indicates that the **BPDC2** nanoparticles are capable to
20 accomplish better cell growth inhibition in cancer cells rather than normal cells. The main
21 hurdle in the use of free CBL as a chemotherapeutic agent is represented by its very poor
22 water solubility though it has clinical importance in the treatment of Non-Hodgkin
23 Lymphoma.⁵⁵ Hence, the higher toxicity of the above mentioned pH-sensitive water-soluble
24 **BPDC2** nanoparticles compared to the **BPC** towards the malignant cells provides a direct
25 evidence that our newly engineered alternating brush copolymer can behave as an efficient
26 drug delivery vehicle for the hydrophobic drugs, such as chlorambucil.
27
28
29
30
31
32
33
34
35
36
37
38
39
40
41
42
43
44
45
46
47
48
49
50
51
52
53
54
55
56
57
58
59
60

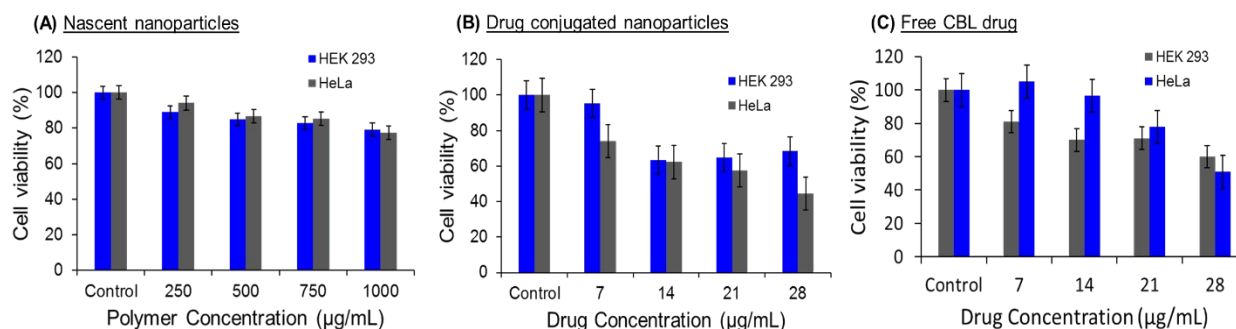


Figure 6. MTT cytotoxicity assay of nascent **BPC** nanoparticle (A), **BPDC2** nanoparticle (B), free CBL (C) in both HEK 293 and HeLa cell lines.

Cellular internalization of BPDC2. Encouraged by the autofluorescent behavior, we examined the cellular internalization of **BPDC2** towards HeLa and MCF-7 cells by fluorescence microscopy. For this purpose, HeLa and MCF-7 cells were incubated with **BPDC2** for 24 h at 37 °C. The CBL concentration used for the treatment was 14 µg/mL with respect to 500 µg/mL nano-scaffold. We observed blue, green and red emissions in both the cell membrane on excitation in blue, green and red channels, respectively (Figure 7). The fluorescence microscope images captured in both the cells strongly suggest the efficient internalization and accumulation of CBL conjugated nanocarrier in the peri-nuclear region, where the intracellular release of CBL takes place upon degradation of ester linkages by means of intracellular stimuli in the cancerous cells, confirmed by the above pH-responsive *in vitro* release studies and MTT assay. Furthermore, the fluorescence images of HeLa cells incubated with **BPDC2** for 10 h were recorded (Figure S13). The comparison of these fluorescence images revealed that the cellular internalization of **BPDC2** at 10 h is similar to those of 24 h. This result implies that the autofluorescent polymeric nanoparticle was capable of undergoing cleavage into the cells within 10 h of incubation.

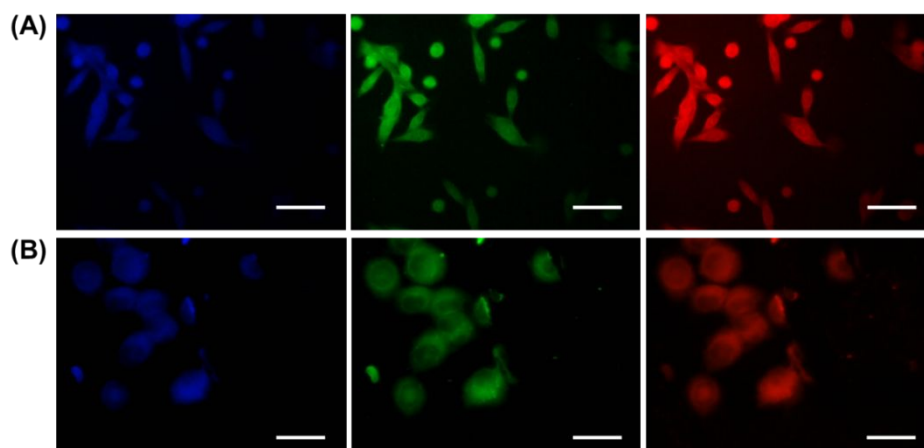


Figure 7. Epifluorescence images of HeLa (A) and MCF-7 (B) cells incubated with **BPDC2** for 24 h, in blue, green and red channels. Scale bar is 10 μm .

Alkylating activity assessment of BPDC2. The NBP assay is a suitable technique to evaluate the activity of alkylating agents.^{30,56} The NBP can serve as a DNA model, because of the similar reactivity of NBP and *N7* position of guanine in DNA.^{57,58} This method is based on the formation of a new chromophore, resulting from the reaction between the alkylating agent (CBL) and the nucleophile, NBP (Figure 8A). Moreover, the nucleophilicity constant of NBP and *N7* position of guanine is almost identical (3.5-3.6), as determined by Swain-Scott nucleophilicity relationship.³⁰ Since CBL is known to alkylate DNA through the reaction at the *N7* position of guanine, we used NBP assay to analyse the alkylating activity of CBL conjugated copolymer **BPDC2**. UV-Vis spectroscopic measurements were carried out for the determination of activity of **BPDC2** towards alkylation in water as a sole solvent during the course of the reaction, which potentially increases the similarity of the assay condition with the biological systems. We have prepared various concentrations of **BPDC2** in water and a particular amount of NBP (in acetone) was added followed by addition of 1.0 mL NaOAc buffer to each reaction mixture. Then the solutions are allowed to heat at 100 $^{\circ}\text{C}$ for 20 min. After cooling at room temperature, a violet colour product was formed upon

basification with triethylamine (Figure 8A). It is observed that the colour intensity and the absorbance of the solutions increased upon increasing the polymer concentration as shown in Figure S14 and Figure 8B, respectively, which shows a linear increase of absorbance as a function of concentration (see inset in Figure 8B). Thus, we inferred that the coloured adduct obeys the Lambert-Beer's law. The colour of the alkylated NBP-CBL adduct was stable up to 6 h at room temperature. However, it should be noted that polymer without drug (CBL) conjugation (**BPC**) does not form any colour on reaction with NBP (data not shown), signifying the utility of CBL moiety in **BPDC2** as an alkylating agent.

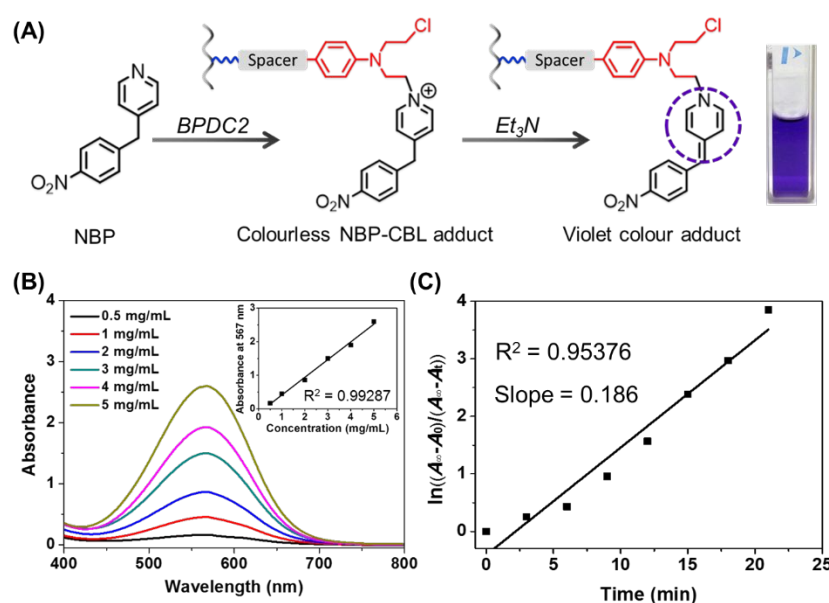


Figure 8. (A) Schematic representation illustrating the S_N2 reaction between NBP and CBL conjugated **BPDC2** polymer. (B) Evolvement of absorption spectra with the increase of polymer concentration. (C) Pseudo-first-order kinetic plot of NBP alkylation.

To understand the alkylation mechanism by NBP, we performed a kinetic study of the reaction. Using a time-dependent analysis at a particular concentration of **BPDC2** (1.0 mg/mL), we found that initially the absorbance increases with time and it becomes saturated indicating no further alkylation after 25 min (Figure S15). In order to determine the rate constant of the reaction, the absorbance values are plotted versus time. The rate constant of

1
2
3 the reaction was calculated by using the equation (1).⁵⁹ As illustrated in Figure 8C, the NBP
4 alkylation reaction follows pseudo-first-order kinetics. The rate constant is estimated to be
5
6 0.186 min⁻¹, which is much higher as compared to only CBL and other derivatives of CBL.⁶⁰
7
8 This is presumably due to the existence of a higher number of pendent CBL entity in the
9
10 copolymer chain. Thus, the newly synthesized CBL conjugated luminescent copolymer has
11
12 better alkylation power compared to the free CBL.
13
14
15
16
17
18
19

20 CONCLUSIONS

21
22
23
24 In summary, the present strategy demonstrates the synthesis of an autofluorescent brush
25
26 copolymer, where anticancer aromatic nitrogen mustard drug CBL is conjugated to the
27
28 polymer side-chain through pH sensitive bonds that are stable at physiological pH 7.4 but are
29
30 cleavable in the mildly acidic pH (corresponding to the endolysosomal pH) and releases
31
32 CBL. The strictly alternating placement of **M1** and **M2** along the polymer main chain leads to
33
34 photoluminescence under UV light irradiation *via* “through-space” π - π interaction between
35
36 the C=O group of maleimide unit and adjacent benzene ring of the styrenic monomer.^{26,27}
37
38 Thus, the brush copolymer is capable of showing blue, green and red emission under UV
39
40 light irradiation albeit it does not consist of any traditional fluorophore moiety.
41
42
43
44

45 The correct amphiphilicity of the copolymer chains assists them to self-assemble into
46
47 nanoparticles in aqueous media and the morphology of self-assembled nanoparticles could be
48
49 tuned by changing the polymer chain length.⁶¹ The nascent nanoparticle (without drug
50
51 conjugation) is nontoxic to both normal (HEK 293) and cancer (HeLa) cells, may be due to
52
53 the presence of densely grafted biocompatible PEG chains. Interestingly, the **BPDC2**
54
55 nanoparticle exhibited superior cell killing and high affectivity to impart toxicity into the
56
57 cancer cells rather than into the normal cells, probably due to acid catalyzed ester hydrolysis
58
59
60

1
2
3 and release of CBL in the acidic environment of cancer cells. The NBP colorimetric assay in
4 the aqueous medium provided a clear evidence on the proficiency of the CBL alkylating
5 agent functionalized **BPDC2** copolymer for DNA alkylation. Because of the
6 autofluorescence in the copolymer, fluorescence microscope imaging could be successfully
7 performed for intracellular tracking of **BPDC2**. Thus, the present study offers delivery and
8 monitoring of intracellular drug delivery of clinically approved nonfluorescent aromatic
9 nitrogen mustard drug CBL, although no fluorescence moiety is integrated into the present
10 DDS. This feature differentiates them from traditional DDS where the systems mainly deal
11 with the fluorescent drug, doxorubicin (DOX).⁶² We believe that this approach may open a
12 new avenue to accomplish intracellular drug delivery of clinically approved nonfluorescent
13 drugs by using autofluorescent polymeric materials.
14
15
16
17
18
19
20
21
22
23
24
25
26
27
28
29
30
31

32 ASSOCIATED CONTENT

33 Supporting information

34 Detailed synthetic methods of monomers including detailed synthetic methods and ¹H NMR
35 spectra of all the intermediates for the synthesis of **M1** and **M2**, ESI-MS spectra of **M1**, SEC
36 traces of brush copolymers, MALDI analysis of **BPDC2**, UV-Vis spectra of **BPDC2**
37 polymer, fluorescence microscope images of **BPDC2**, self-assembly study of copolymer by
38 ¹H NMR, degradation study of self-assembled nanoparticles at pH 7.4, fluorescence images
39 of HeLa cells incubated with **BPDC2** for 10 h, digital photographs of alkylated NBP-CBL
40 adduct, time-dependent NBP alkylation assay. This material is available free of charge *via* the
41 Internet at <http://pubs.acs.org>.
42
43
44
45
46
47
48
49
50
51
52
53
54
55
56
57
58
59
60

1
2
3 AUTHOR INFORMATION
4

5 **Corresponding Author**
6

7 * E-mail: p_de@iiserkol.ac.in
8
9

10
11
12 **ACKNOWLEDGMENTS**
13

14 The authors thank Dr. Sankar Maiti (Department of Biological Sciences, Indian Institute of
15 Science Education and Research Kolkata) for providing cell culture facility and fruitful
16 suggestions during the manuscript preparation. B.S. acknowledges Council of Scientific and
17 Industrial Research (CSIR), Government of India, India, for his senior research fellowship
18 (SRF). S.S. acknowledges Science and Engineering Research Board (SERB) for her National
19 Post-doctoral Fellow (NPDF) fellowship.
20
21
22
23
24
25
26
27
28
29
30
31

32 **REFERENCES**
33

- 34 (1) Danhier, F.; Feron, O.; Préat, V. To Exploit the Tumor Microenvironment: Passive and
35 Active Tumor Targeting of Nanocarriers for Anti-Cancer Drug Delivery. *J. Controlled*
36 *Release* **2010**, *148*, 135-146.
37
38 (2) Liu, J.; Pang, Y.; Zhu, Z.; Wang, D.; Li, C.; Huang, W.; Zhu, X.; Yan, D. Therapeutic
39 Nanocarriers with Hydrogen Peroxide-Triggered Drug Release for Cancer Treatment.
40 *Biomacromolecules* **2013**, *14*, 1627-1636.
41
42 (3) Kondo, N.; Takahashi, A.; Ono, K.; Ohnishi, T. DNA Damage Induced by Alkylating
43 Agents and Repair Pathways. *J. Nucleic Acids* **2010**, *2010*, 543531-543537.
44
45 (4) Polavarapu, A.; Stillabower, J. A.; Stubblefield, S. G. W.; Taylor, W. M.; Baik, M.-H.
46 The Mechanism of Guanine Alkylation by Nitrogen Mustards: A Computational Study. *J.*
47 *Org. Chem.* **2012**, *77*, 5914-5921.
48
49
50
51
52
53
54
55
56
57
58
59
60

- 1
2
3
4 (5) Robak, T.; Kasznicki, M. Alkylating Agents and Nucleoside Analogues in the Treatment
5 of B Cell Chronic Lymphocytic Leukemia. *Leukemia* **2002**, *16*, 1015-1027.
6
7
8
9 (6) Omoomi, F. D.; Siadat, S. D.; Nourmohammadi, Z.; Tabasi, M. A.; Pourhoseini, S.;
10 Babael, R. A.; Saffari, M.; Ardestani, M. S. Molecular Chlorambucil-Methionine Conjugate:
11 Novel Anti-Cancer Agent Against Breast MCF-7 Cell Model. *J. Cancer Sci. Ther.* **2013**, *5*,
12 075-084.
13
14
15
16
17
18 (7) Saha, B.; Haldar, U.; De, P. Polymer-Chlorambucil Drug Conjugates: A Dynamic
19 Platform of Anticancer Drug Delivery. *Macromol. Rapid Commun.* **2016**, *37*, 1015-1020.
20
21
22
23 (8) Jana, A.; Nguyen, K. T.; Li, X.; Zhu, P.; Tan, N. S.; Ågren, H.; Zhao, Y. Perylene-
24 Derived Single-Component Organic Nanoparticles with Tunable Emission: Efficient
25 Anticancer Drug Carriers with Real-Time Monitoring of Drug Release. *ACS Nano* **2014**,
26 *8*, 5939-5952.
27
28
29
30
31
32 (9) Barman, S.; Mukhopadhyay, S. K.; Gangopadhyay, M.; Biswas, S.; Dey, S.; Singh, N. D.
33 P. Coumarin–Benzothiazole–Chlorambucil (Cou–Benz–Cbl) Conjugate: An ESIPT Based pH
34 Sensitive Photoresponsive Drug Delivery System. *J. Mater. Chem. B* **2015**, *3*, 3490-3497.
35
36
37
38
39 (10) Barman, S.; Das, J.; Biswas, S.; Maiti, T. K.; Singh, N. D. P. A Spiropyran–Coumarin
40 Platform: An Environment Sensitive Photoresponsive Drug Delivery System for Efficient
41 Cancer Therapy. *J. Mater. Chem. B* **2017**, *5*, 3940-3944.
42
43
44
45
46 (11) Venkatesh, Y.; Karthik, S.; Rajesh, Y.; Mandal, M.; Jana, A.; Singh, N. D. P. Three-
47 Arm, Biotin-Tagged Carbazole–Dicyanovinyl–Chlorambucil Conjugate: Simultaneous
48 Tumor Targeting, Sensing, and Photoresponsive Anticancer Drug Delivery. *Chem. Asian J.*
49 **2016**, *11*, 3482-3486.
50
51
52
53
54
55 (12) Cunningham, C. W.; Mukhopadhyay, A.; Lushington, G. H.; Blagg, B. S. J.; Prisinzano,
56 T. E.; Krise, J. P. Uptake, Distribution and Diffusivity of Reactive Fluorophores in Cells:
57 Implications Toward Target Identification. *Mol. Pharmaceutics.* **2010**, *7*, 1301-1310.
58
59
60

-
- 1
2
3
4 (13) Ulbrich, K.; Holá, K.; Šubr, V.; Bakandritsos, A.; Tuček, J.; Zbořil, R. Targeted Drug
5
6 Delivery with Polymers and Magnetic Nanoparticles: Covalent and Noncovalent Approaches,
7
8 Release Control, and Clinical Studies. *Chem. Rev.* **2016**, *116*, 5338-5431.
9
10
11 (14) Kanamala, M.; Wilson, W. R.; Yang, M.; Palmer, B. D.; Wu, Z. Mechanisms and
12
13 Biomaterials in pH-Responsive Tumour Targeted Drug Delivery: A Review. *Biomaterials*
14
15 **2016**, *85*, 152-167.
16
17
18 (15) Johnson, R. P.; Jeong, Y. -Il.; John, J. V.; Chung, C.-W.; Kang, D. H.; Selvaraj, M.;
19
20 Suh, H.; Kim, I. Dual Stimuli-Responsive Poly(*N*-isopropylacrylamide)-*b*-Poly(L-histidine)
21
22 Chimeric Materials for the Controlled Delivery of Doxorubicin into Liver Carcinoma.
23
24 *Biomacromolecules* **2013**, *14*, 1434-1443.
25
26
27 (16) Wang, L.; Liu, G.; Wang, X.; Hu, J.; Zhang, G.; Liu, S. Acid-Disintegratable
28
29 Polymersomes of pH-Responsive Amphiphilic Diblock Copolymers for Intracellular Drug
30
31 Delivery. *Macromolecules* **2015**, *48*, 7262-7272.
32
33
34 (17) Mukherjee, S.; Sarma, J. D.; Shunmugam, R. pH-Sensitive Nanoaggregates for Site-
35
36 Specific Drug-Delivery as well as Cancer Cell Imaging. *ACS Omega* **2016**, *1*, 755-764.
37
38
39 (18) Li, D.; Bu, Y.; Zhang, L.; Wang, X.; Yang, Y.; Zhuang, Y.; Yang, F.; Shen, H.; Wu, D.
40
41 Facile Construction of pH- and Redox-Responsive Micelles from a Biodegradable Poly(β -
42
43 hydroxyl amine) for Drug Delivery. *Biomacromolecules* **2016**, *17*, 291-300.
44
45
46 (19) Kashyap, S.; Singh, N.; Surnar, B.; Jayakannan, M. Enzyme and Thermal Dual
47
48 Responsive Amphiphilic Polymer Core-Shell Nanoparticle for Doxorubicin Delivery to
49
50 Cancer Cells. *Biomacromolecules* **2016**, *17*, 384-398.
51
52
53 (20) Wang, D.; Imae, T. Fluorescence Emission from Dendrimers and its pH Dependence. *J.*
54
55 *Am. Chem. Soc.* **2004**, *126*, 13204-13205.
56
57
58
59
60

- 1
2
3
4 (21) Sun, M.; Hong, C.-Y.; Pan, C.-Y. A Unique Aliphatic Tertiary Amine Chromophore:
5 Fluorescence, Polymer Structure, and Application in Cell Imaging. *J. Am. Chem. Soc.* **2012**,
6 *134*, 20581-20584.
7
8
9
10
11 (22) Lin, Y.; Gao, J.-W.; Liu, H.-W.; Li, Y.-S. Synthesis and Characterization of
12 Hyperbranched Poly(ether amide)s with Thermoresponsive Property and Unexpected Strong
13 Blue Photoluminescence. *Macromolecules* **2009**, *42*, 3237-3246.
14
15
16
17
18 (23) Zhao, E.; Lam, J. W. Y.; Meng, L.; Hong, Y.; Deng, H.; Bai, G.; Huang, X.; Hao, J.;
19 Tang, B. Z. Poly[(maleic anhydride)-*alt*-(vinyl acetate)]: A Pure Oxygenic Nonconjugated
20 Macromolecule with Strong Light Emission and Solvatochromic Effect. *Macromolecules*
21 **2015**, *48*, 64-71.
22
23
24
25
26
27 (24) Ru, Y.; Zhang, X.; Song, W.; Liu, Z.; Feng, H.; Wang, B.; Guo, M.; Wang, X.; Luo, C.;
28 Yang, W.; Li, Y.; Qiao, J. A New Family of Thermoplastic Photoluminescence Polymers.
29 *Polym. Chem.* **2016**, *7*, 6250-6256.
30
31
32
33
34 (25) Henry, S. M.; El-Sayed, M. E. H.; Pirie, C. M.; Hoffman, A. S.; Stayton, P. S. pH-
35 Responsive Poly(styrene-*alt*-maleic anhydride) Alkylamide Copolymers for Intracellular
36 Drug Delivery. *Biomacromolecules* **2006**, *7*, 2407-2414.
37
38
39
40
41 (26) Saha, B.; Bauri, K.; Bag, A.; Ghorai, P. K.; De, P. Conventional Fluorophore-Free Dual
42 pH- and Thermo-Responsive Luminescent Alternating Copolymer. *Polym. Chem.* **2016**, *7*,
43 6895-6900.
44
45
46
47 (27) Bauri, K.; Saha, B.; Mahanti, J.; De, P. A Nonconjugated Macromolecular Luminogen
48 for Speedy, Selective and Sensitive Detection of Picric Acid in Water. *Polym. Chem.* **2017**, *8*,
49 7180-7187.
50
51
52
53
54 (28) Benhabbour, R. S.; Sheardown, H.; Adronov, A. Protein Resistance of PEG-
55 Functionalized Dendronized Surfaces: Effect of PEG Molecular Weight and Dendron
56 Generation. *Macromolecules* **2008**, *41*, 4817-4823.
57
58
59
60

-
- 1
2
3
4 (29) Otsuka, H.; Nagasaki, Y.; Kataoka, K. PEGylated Nanoparticles for Biological and
5
6
7
8
9
10
11
12
13
14
15
16
17
18
19
20
21
22
23
24
25
26
27
28
29
30
31
32
33
34
35
36
37
38
39
40
41
42
43
44
45
46
47
48
49
50
51
52
53
54
55
56
57
58
59
60
- (29) Otsuka, H.; Nagasaki, Y.; Kataoka, K. PEGylated Nanoparticles for Biological and Pharmaceutical Applications. *Adv. Drug Delivery Rev.* **2012**, *64*, 246-255.
- (30) Gómez-Bombarelli, R.; González-Pérez, M.; Calle, E.; Casado, J. Potential of the NBP Method for the Study of Alkylation Mechanisms: NBP as a DNA-Model. *Chem. Res. Toxicol.* **2012**, *25*, 1176-1191.
- (31) Provencher, P. A.; Love, J. A. Synthesis and Performance of a Biomimetic Indicator for Alkylating Agents. *J. Org. Chem.* **2015**, *80*, 9603-9609.
- (32) G. Odian, Principles of Polymerization, Fourth Edition, New Jersey, John Wiley & Sons, Inc., **2004**.
- (33) Su, L.; Wang, C.; Polzer, F.; Lu, Y.; Chen, G.; Jiang, M. Glyco-Inside Micelles and Vesicles Directed by Protection–Deprotection Chemistry. *ACS Macro Lett.* **2014**, *3*, 534-539.
- (34) York, A. W.; Kirkland, S. E.; McCormick, C. L. Advances in the Synthesis of Amphiphilic Block Copolymers *via* RAFT Polymerization: Stimuli-Responsive Drug and Gene Delivery. *Adv. Drug Delivery Rev.* **2008**, *60*, 1018-1036.
- (35) Kakkar, A.; Traverso, G.; Farokhzad, O. C.; Weissleder, R.; Langer, R. Evolution of Macromolecular Complexity in Drug Delivery Systems. *Nat. Rev. Chem.* **2017**, *1*, 0063.
- (36) Lutz, J.-F.; Ouchi, M.; Liu, D. R.; Sawamoto, M. Sequence-Controlled Polymers. *Science* **2013**, *341*, 1238149.
- (37) Huang, J.; Turner, S. R. Recent Advances in Alternating Copolymers: The Synthesis, Modification, and Applications of Precision Polymers. *Polymer* **2017**, *116*, 572–586.
- (38) Mohamed, M. G.; Hsu, H. C.; Hong, J. L.; Kuo, S. W. Unexpected Fluorescence from Maleimide Containing Polyhedral Oligomeric Silsesquioxanes: Nanoparticle and Sequence Distribution Analyses of Polystyrene-Based Alternating Copolymers. *Polym. Chem.* **2016**, *7*, 135-145.

- 1
2
3
4 (39) Li, W.; Che, C.; Pang, J.; Cao, Z.; Jiao, Y.; Xu, J.; Ren, Y.; Li, X. Autofluorescent
5
6 Polymers: 1H,1H,2H,2H-Perfluoro-1-decanol Grafted Poly(styrene-*b*-acrylic acid) Block
7
8 Copolymers without Conventional Fluorophore. *Langmuir* **2018**, *34*, 5334-5341.
- 9
10
11 (40) Du, J.-Z.; Tang, L.-Y.; Song, W.-J.; Shi, Y.; Wang, J. Evaluation of Polymeric Micelles
12
13 from Brush Polymer with Poly(ϵ -caprolactone)-*b*-Poly(ethylene glycol) Side Chains as Drug
14
15 Carrier. *Biomacromolecules* **2009**, *10*, 2169-2174.
- 16
17
18 (41) Li, Z.; Ma, J.; Lee, N. S.; Wooley, K. L. Dynamic Cylindrical Assembly of Triblock
19
20 Copolymers by a Hierarchical Process of Covalent and Supramolecular Interactions. *J. Am.*
21
22 *Chem. Soc.* **2011**, *133*, 1228-1231.
- 23
24
25 (42) Zou, J.; Yu, Y.; Li, Y.; Ji, W.; Chen, C.-K.; Law, W.-C.; Prasad, P. N.; Cheng, C. Well-
26
27 Defined Diblock Brush Polymer-Drug Conjugates for Sustained Delivery of Paclitaxel.
28
29 *Biomater. Sci.* **2015**, *3*, 1078-1084.
- 30
31
32 (43) Ji, X.; Li, Y.; Wang, H.; Zhao, R.; Tang, G.; Huang, F. Facile Construction of Fluorescent
33
34 Polymeric Aggregates with Various Morphologies by Self-Assembly of Supramolecular
35
36 Amphiphilic Graft Copolymers. *Polym. Chem.* **2015**, *6*, 5021-5025.
- 37
38
39 (44) Shi, Y.; Cardoso, R. M.; van Nostrum, C. F.; Hennink, W. E. Anthracene Functionalized
40
41 Thermosensitive and UV-Crosslinkable Polymeric Micelles. *Polym. Chem.* **2015**, *6*, 2048-
42
43 2053.
- 44
45
46 (45) Pal, S.; Roy, S. G.; De, P. Synthesis *via* RAFT Polymerization of Thermo- and pH-
47
48 Responsive Random Copolymers Containing Cholic Acid Moieties and Their Self-Assembly
49
50 in Water. *Polym. Chem.* **2014**, *5*, 1275-1284.
- 51
52
53 (46) Petros, R. A.; DeSimone, J. M. Strategies in the Design of Nanoparticles for Therapeutic
54
55 Applications. *Nat. Rev. Drug Discovery* **2010**, *9*, 615-627.
- 56
57
58 (47) Son, H. N.; Srinivasan, S.; Yhee, J. Y.; Das, D.; Daugherty, B. K.; Berguig, G. Y.;
59
60 Oehle, V. G.; Kim, S. H.; Kim, K.; Kwon, I. C.; Stayton, P. S.; Convertine, A. J.

1
2
3
4
5
6
7
8
9
10
11
12
13
14
15
16
17
18
19
20
21
22
23
24
25
26
27
28
29
30
31
32
33
34
35
36
37
38
39
40
41
42
43
44
45
46
47
48
49
50
51
52
53
54
55
56
57
58
59
60

Chemotherapeutic Copolymers Prepared *via* the RAFT Polymerization of Prodrug Monomers. *Polym. Chem.* **2016**, *7*, 4494-4505.

(48) Giacomelli, F.C.; Stepánek, P.; Giacomelli, C.; Schmidt, V.; Jäger, E.; Jäger, A.; Ulbrich, K. pH-Triggered Block Copolymer Micelles Based on a pH-Responsive PDPA (Poly[2-(diisopropylamino)ethyl methacrylate]) Inner Core and a PEO (Poly(Ethylene Oxide)) Outer Shell as a Potential Tool for the Cancer Therapy. *Soft Matter* **2011**, *7*, 9316-9325.

(49) Ganivada, M. N.; Kumar, P.; Babu, A.; Sarma, J. D.; Shunmugam, R. Engineering a New Class of Multiarm Homopolymer for Sustainable Drug Delivery. *ACS Biomater. Sci. Eng.* **2017**, *3*, 903-908.

(50) Schoenmakers, R. G.; van de Wetering, P.; Elbert, D. L.; Hubbell, J. A. The Effect of the Linker on the Hydrolysis Rate of Drug-Linked Ester Bonds. *J. Controlled Release* **2004**, *95*, 291-300.

(51) Bej, R.; Sarkar, J.; Ray, D.; Aswal, V. K.; Ghosh, S. Morphology Regulation in Redox Destructible Amphiphilic Block Copolymers and Impact on Intracellular Drug Delivery. *Macromol. Biosci.* **2018**, *18*, 1800057 (1-10).

(52) Das, D.; Srinivasan, S.; Kelly, A. M.; Chiu, D. Y.; Daugherty, B. K.; Ratner, D. M.; Stayton, P. S.; Convertine, A. J. RAFT Polymerization of Ciprofloxacin Prodrug Monomers for the Controlled Intracellular Delivery of Antibiotics. *Polym. Chem.* **2016**, *7*, 826-837.

(53) Pramod, P. S.; Takamura, K.; Chaphekar, S.; Balasubramanian, N.; Jayakannan, M. Dextran Vesicular Carriers for Dual Encapsulation of Hydrophilic and Hydrophobic Molecules and Delivery into Cells. *Biomacromolecules* **2012**, *13*, 3627-3640.

(54) Fang, J.; Nakamura, H.; Maeda, H. The EPR effect: Unique Features of Tumor Blood Vessels for Drug Delivery, Factors Involved, and Limitations and Augmentation of the Effect. *Adv. Drug Delivery Rev.* **2011**, *63*, 136-151.

(55) Guaragna, A.; Chiaviello, A.; Paoletta, C.; D'Alonzo, D.; Palumbo, G. Synthesis and Evaluation of Folate-Based Chlorambucil Delivery Systems for Tumor-Targeted Chemotherapy. *Bioconjugate Chem.* **2012**, *23*, 84-96.

(56) Wheeler, G. P.; Chumley, S. Alkylating Activity of 1,3-Bis(2-chloroethyl)-1-nitrosourea and Related Compounds. *J. Med. Chem.* **1967**, *10*, 259-261.

(57) Cespedes-Camacho, I. F.; Manso, J. A.; Gonzalez-Jimenez, M.; Casado, E. C. J. The Reactivity of Vinyl Compounds as Alkylating Agents. *Monatsh. Chem.* **2012**, *143*, 723-727.

(58) Chmielewicz, Z. F.; Fiel, R. J.; Bardos, T. J.; Ambrus, J. L. Alterations of Some Macromolecular and Biochemical Properties of Calf Thymus DNA Caused by Dual Antagonists and Nitrogen Mustard. *Cancer Res.* **1967**, *27*, 1248-1257.

(59) Fernández-Rodríguez, E.; Manso, J. A.; Pérez-Prior, M. T.; García-Santos, M. D. P.; Calle, E.; Casado, J. The Unusual Ability of α -angelicalactone to form Adducts: A Kinetic Approach. *Int. J. Chem. Kinet.* **2007**, *39*, 591-594.

(60) Fedeles, B. I.; Zhu, A. Y.; Young, K. S.; Hillier, S. M.; Proffitt, K. D.; Essigmann, J. M.; Croy, R. G. Chemical Genetics Analysis of an Aniline Mustard Anticancer Agent Reveals Complex I of the Electron Transport Chain as a Target. *J. Biol. Chem.* **2011**, *286*, 33910-33920.

(61) Haldar, U.; Nandi, M.; Ruidas, B.; De, P. Controlled Synthesis of Amino-Acid Based Tadpole-Shaped Organic/Inorganic Hybrid Polymers and Their Self-Assembly in Aqueous Media. *Eur. Polym. J.* **2015**, *67*, 274-283.

(62) Yu, Y.; Chen, C.-K.; Law, W.-C.; Sun, H.; Prasad, P. N.; Cheng, C. A Degradable Brush Polymer-Drug Conjugate for pH-Responsive Release of Doxorubicin. *Polym. Chem.* **2015**, *6*, 953-961.

1
2
3
4
5
6
7
8 **For “Table of Contents” Use Only**

9
10
11 **Aromatic Nitrogen Mustard-Based Autofluorescent Amphiphilic Brush Copolymer as**
12 **pH-Responsive Drug Delivery Vehicle**
13

14
15 Biswajit Saha, Neha Choudhury, Soma Seal, Bhuban Ruidas, and Priyadarsi De*
16
17
18
19

